Directly Derived Non-Hyper-Singular Boundary Integral Equations for Acoustic Problems II: The Collocation Implementation

Z.Y. Qian, Z.D. Han, P. Ufimtsev, and S.N. Atluri[1]

Summary

The weak-form of Helmholtz differential equation, in conjunction with vector test-functions, which are gradients of the fundamental solutions to the Helmholtz differential equation in free space, is utilized as the basis in order to directly derive non-hyper-singular boundary integral equations for the velocity potential, as well as its gradients. Several basic identities governing the fundamental solution to the Helmholtz differential equation for velocity potential, are also derived for the further desingularization of the strongly singular integral equations for the potential and its gradients to be only weakly-singular.

Introduction

In the present paper, without directly differentiating the derivatives of the conventional boundary integral equation for the potential, which will result in the hyper-singular integrals, novel non-hyper-singular boundary integral equations are derived directly, for the gradients of the velocity potential. The acoustic potential gradients are related to the sound velocity in their physical meaning. The basic idea of using the gradients of the fundamental solution to the Helmholtz differential equation, as *vector test-functions* to write the weak-form of the original Helmholtz differential equation, and thereby directly derive a *non-hyper-singular boundary integral equations for velocity potential gradients*, which use the displacement and velocity gradients to directly establish the displacement and displacement gradient boundary integral equations in elastic/plastic solid problems, as well as traction boundary integral equations [1],[2], which are very simple to be implemented numerically.

The boundary integral equations for the potential [labeled here as ϕ-BIE], and its gradient [labeled here as q-BIE], which are newly presented in the present paper, are only strongly singular [$O(r^{-2})$]. These *strongly singular* ϕ-BIE, and q-BIE are further regularized to *only weakly singular* [$O(r^{-1})$] types, which are labeled here as R-ϕ-BIE, R-q-BIE, respectively. This is achieved *by using certain basic identities of the fundamental solution of the Helmholtz differential equation for potential*. In addition, general Petrov-Galerkin based methods can be formulated as shown in [3] to solve the R-ϕ-BIE, and R-q-BIE, in their weak senses. With this general Petrov-Galerkin formulation, one can

[1] Center for Aerospace Research \& Education, University of California, Irvine, Irvine, CA. 92612, USA

easily derive different methods, such as the (Symmetric Galerkin Boundary Element Method) SGBEM-R-[ϕ & q]-BIE, by using various alternative functions as the test function. In the present boundary integral equations, *C^0 continuity of ϕ as well as q over the boundary elements is sufficient for numerical implementation*. Through following the general Petrov-Galerkin formulation, there will result in a family of methods.

Collocation implementation of the BIE's Petrov Galerkin scheme

As what we state in [3], if the test function $w(\mathbf{x})$ is chosen as a Dirac delta function, i.e., $w(\mathbf{x}) = \delta(\mathbf{x}, \mathbf{x}_m)$ at $\partial\Omega$, we obtain the standard "collocation" boundary element method. [BEM-R-ϕ &q-BIE]

$$\begin{aligned}&\int_{\partial\Omega} q(\xi)\phi^*(\mathbf{x},\xi)dS - \int_{\partial\Omega}[\phi(\xi)-\phi(\mathbf{x})]\Theta^*(\mathbf{x},\xi)dS \\ &= \int_{\partial\Omega}^{CPV}\Theta^*(\mathbf{x},\xi)\phi(\mathbf{x})dS + \frac{1}{2}\phi(\mathbf{x})\end{aligned} \qquad \mathbf{x}\in\partial\Omega \quad (1)$$

in which $\phi(\xi)-\phi(\mathbf{x})$ becomes $\mathrm{O}(r)$ when $\xi\to\mathbf{x}$, and Eq. (1) becomes weakly-singular. Eq. (1) is labeled as BEM-R-ϕ-BIE. And the BEM-R-q-BIE can be obtained as:

$$\begin{aligned}-\frac{1}{2}q(\mathbf{x}) &= \int_{\partial\Omega}[q(\xi)-n_i(\xi)\psi_i(\mathbf{x})]\hat{\Theta}^*(\mathbf{x},\xi)dS + \int_{\partial\Omega}k^2 n_k(\mathbf{x})n_k(\xi)\phi(\xi)\phi^*(\mathbf{x},\xi)dS \\ &+ \int_{\partial\Omega}[D_t\phi(\xi)-(D_t\phi)(\mathbf{x})]n_k(\mathbf{x})e_{ikt}\phi^*_{,i}(\mathbf{x},\xi)dS + \int_{\partial\Omega}^{CPV}\Theta^*(\mathbf{x},\xi)q(\mathbf{x})dS\end{aligned} \quad (2)$$

where the kernel function $\hat{\Theta}^*(\mathbf{x},\xi) = -\dfrac{\partial\phi^*(\mathbf{x},\xi)}{\partial n_x} = n_k(\mathbf{x})\dfrac{\partial\phi^*(\mathbf{x},\xi)}{\partial\xi_k}$ at $\xi\in\partial\Omega$. Suppose $\partial\Omega$ is smooth; then $[q(\xi)-n_i(\xi)\psi_i(\mathbf{x})]$ and $[D_t\phi(\xi)-(D_t\phi)(\mathbf{x})]$ become $O(r)$ when $\xi\to\mathbf{x}$, and Eq. (2) becomes weakly singular [$O(r^{-1})$] on a 3D problem. On the other hand, when $\partial\Omega$ has corners, $[q(\xi)-n_i(\xi)\psi_i(\mathbf{x})]$ and $[D_t\phi(\xi)-(D_t\phi)(\mathbf{x})]$ may become $O(r^{\lambda-1})$ when $\xi\to\mathbf{x}$, and thus, in a theoretical sense, Eq. (2) is no longer weakly singular. However, in a numerical implementation of the R-q-BIE, viz. Eq. (2), directly, *through a collocation process, to derive a qBoundary Element Method (BEM-R-q-BIE)*, we envision using only C^0 polynomial interpolations of ϕ and q. Thus, in the numerical implementation of the BEM-q-BIE by a collocation of (2), we encounter only weakly singular integrals.

Numerical results

The field radiated from a pulsating sphere into the infinite homogeneous medium is chosen as an example for the exterior problem. For the purpose of comparison, BEM-R-[ϕ & q]-BIE and SGBEM-R-[ϕ & q]-BIE, the whole sphere is considered for modeling: a 24 element model and a 64 element model. The models are discretized by using 8-node isoparametric quadrilateral elements. The evaluation of all integrals of kernels is performed by using 3x3 standard Gaussian quadrature.

In Fig. 1 and Fig. 2, the real and imaginary parts of dimensionless surface acoustic pressures are plotted with respect to the reduced frequency *ka*. Fig. 1 presents the numerical solutions with 24 elements, while results with 64 elements are plotted in Fig. 2. The present results are seen to converge to the analytical solution, with a mesh refinement. It is obvious that the conventional BIE method fails to provide unique solutions near $k = \pi, 2\pi \cdots$. The present BEM-R-[ϕ & q]-BIE solutions and exact solution have a good agreement between with *ka* up to 8.0. The accuracy of BEM-R-[ϕ & q]-BIE is lower than that of the SGBEM in the coarse model (24 element) as shown in Fig. 1; however, by refining the mesh size, an acceptable result can be obtained easily with a comparatively low computation cost as shown in Fig. 1, by using BEM-R-[ϕ & q]-BIE. The other method of increasing the accuracy of BEM-R-[ϕ & q]-BIE is to use higher order Gaussian Quadrature. The computational costs shown in Table 1 are based on the MATLAB code running on the desktop with 1.5 GHz Intel Pentium IV CPU, and 512MB Memory. The SGBEM-R-[ϕ & q]-BIE is much slower, because of the double integral evaluation for every element, and the SGBEM's code for evaluating weakly singular integrals is more complicated than in BEM. On the contrary, the BEM-R-[ϕ & q]-BIE only encounters single integral for every element, and therefore, it is faster.

The acoustic scattering of plane incident waves, with a unit amplitude (e^{-ikx}), from a rigid sphere is considered as the second example. The magnitudes of the ratio of $\phi^s(\mathbf{x})$ to $\phi^i(\mathbf{x})$, at r=5a are plotted against the angle, for ka=π. Four discretization models are used here.

Fig. 3 is a comparison of the analytical solution and four element models, in which only regular 8 node quadrilateral elements are used. The solutions show that the method converges, as the number of elements increases, and the BEM-R-[ϕ & q]-BIE solutions have a fairly good agreement with the analytical solution, with the use of a relatively small number of elements. Moreover, the C^0 elements have been demonstrated by this example to give fairly good results for most values of θ except near the forward scattering direction.

Closure

The weak-form of Helmholtz differential equation with vector test-functions is employed, as the basis in the present paper in order to directly derive non-hyper-singular boundary integral equations. Thereby, the difficulties with hyper-singular integrals, involved in the composite Helmholtz integral equations, can be overcome. Further desingularization of the strongly singular integrals to the order of $O(r^{-1})$ is made possible with the use of certain basic identities of the fundamental solution of the Helmholtz differential equation for potential. These new weakly-singular integral equations designated as R-ϕ-BIE and R-q-BIE, respectively, are solved by using direct collocations. The attendant boundary element methods are desingularized as BEM-R-[ϕ & q]-BIE in this paper. There is no requirement of smoothness of the chosen trial functions for ϕ and q, and C^0 continuity is sufficient for numerical implementation.

Fig. 4 compares the element size and wavelength for achieving accuracies with under 5% and 10% error, in pulsating sphere problem by using BEM-R-ϕ-BIE, and BEM-R-q-BIE. The error is measured in the magnitude of the acoustic pressure at r=5a. For the boundary element method, and the finite element method, it is well known that the mesh size has to be less than the wave length of the acoustic wave, in order to obtain an acceptable solution. This is shown in Fig. 4. Further effort will be made in extending the present approach, using the Meshless Local Petrov Galerkin approach, to develop MLPG-R-ϕ-BIE, and MLPG-R-q-BIE, respectively. These MLPG methods are expected to be a good way to improve the mesh size requirement in the numerical methods for solving the present R-[ϕ & q]-BIE.

An alternate approach to cope with very high frequency acoustic radiation and scattering problems is to use the method of asymptotics pioneered by Ufimtsev [2003] in electromagnetics, and is being developed in the context of asymptotics by Ufimtsev and Atluri [2004a, 2004b].

Acknowledgements

The results presented herein were obtained during the course of investigation supported by the US Army Research Laboratory. The useful discussions with Drs. R. Namburu and R. Rajendran are gratefully acknowledged.

References

1. Han, Z.D.; Atluri, S.N. (2003a): On simple formulations of weakly-singular tBIE&dBIE, and Petrov-Galerkin approaches, *CMES: Computer Modeling in Engineering & Sciences*, vol.4, no.1, pp.5-20

2. Han. Z.D.; Atluri, S. N. (2003b): Truly Meshless Local Patrov-Galerkin (MLPG)

solutions of traction & displacement BIEs. *CMES: Computer Modeling in Engineering & Sciences*, vol. 4, pp. 665-678.

3. Okada, H.; Rajiyah, H.; Atluri, S. N. (1989)a: A Novel Displacement Gradient Boundary Element Method for Elastic Stress Analysis with High Accuracy, *J. Applied Mech*., April 1989, pp. 1-9.

4. Okada, H.; Rajiyah, H.; Atluri, S. N. (1989)b: Non-hypersingular integral representations for velocity (displacement) gradients in elastic/plastic solids (small or finite deformations), *Comp. Mech.*, vol. 4, pp. 165-175.

5. Qian, Z.Y.; Han, Z.D.; Atluri, S.N. (2004): Directly Derived Non-Hyper-Singular Boundary Integral Equations for Acoustic Problems, and Their Solution through Petrov-Galerkin Schemes. *CMES: Computer Modeling in Engineering& Sciences*, (in print)

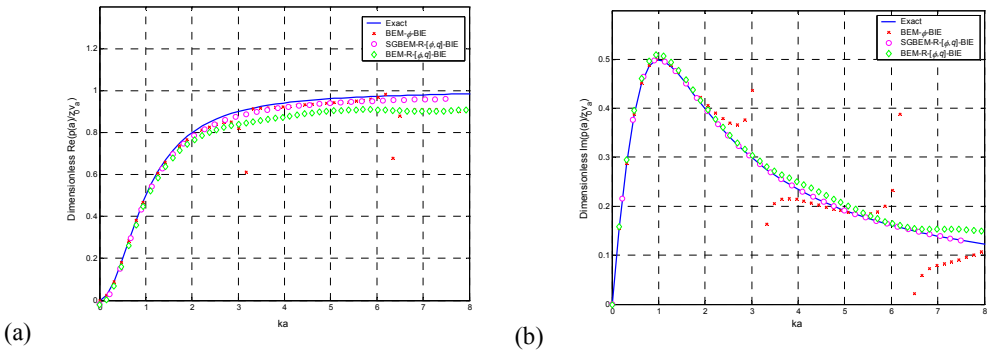

(a) (b)

Fig. 1 Dimensionless surface acoustic pressure of a pulsating (24 elements): (a) real part; (b) imaginary part.

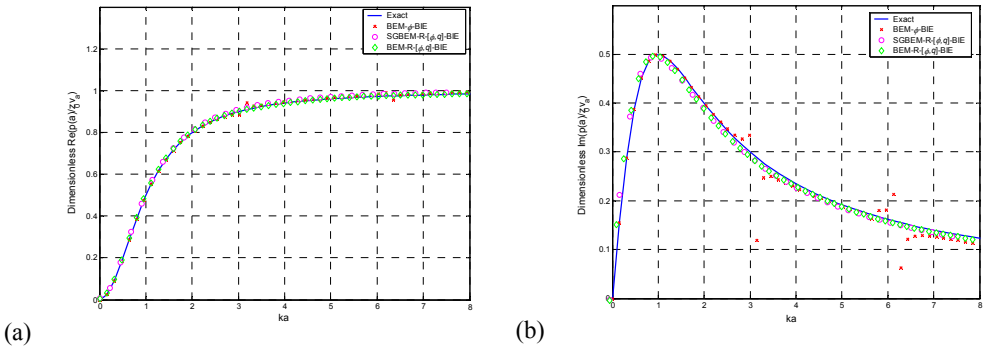

(a) (b)

Fig. 2 Dimensionless surface acoustic pressure of a pulsating sphere (64 elements): (a) real part; (b) imaginary part.

Table 1 The comparison of the computational costs between BEM-R-[ϕ & q]-BIE and SGBEM-R-[ϕ & q]-BIE

	24 Element Model	64 Element Model
BEM-R-[ϕ & q]-BIE	60 s	378 s
SGBEM-R-[ϕ & q]-BIE	284 s	1346 s

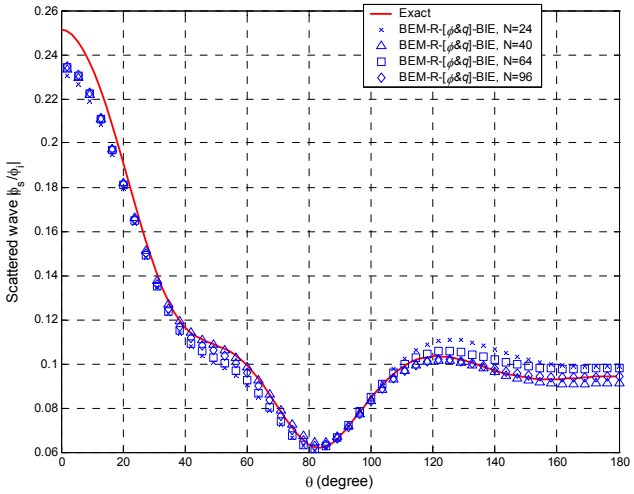

Fig. 3 Scattering from the rigid sphere at r=5a, ka=π; with BEM-R-[ϕ & q]-BIE

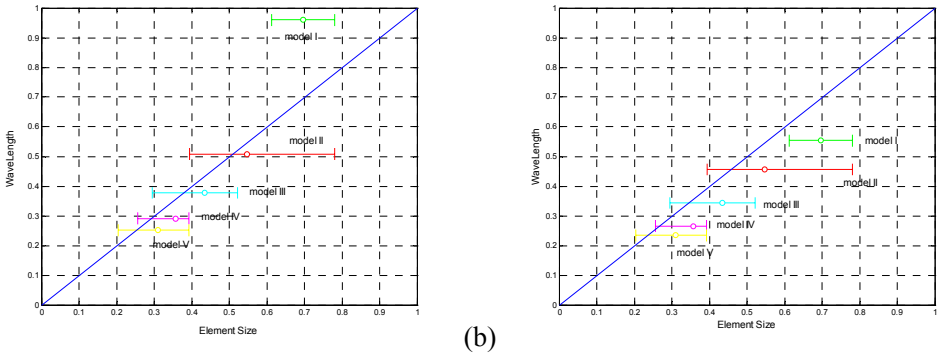

Fig. 4 Relationship between wave length and element size in pulsating sphere case (a) 5% error; (b) 10% error. model I: N=24; II: N=40; III: N=64; IV: N=96; V: N=128.